PERGAMON

International Journal of Multiphase Flow 26 (2000) 1401–1418

International Journal of Multiphase Flow

www.elsevier.com/locate/ijmulflow

Laser Doppler anemometry measurements in an index of refraction matched column in the presence of dispersed beads
Part I

S.J. Haam[a, 1], R.S. Brodkey[a,*], I. Fort[b], L. Klaboch[c], M. Placnik[d], V. Vanecek[e]

[a]*Department of Chemical Engineering, The Ohio State University, 140 West 19th Avenue, Columbus, OH 43210-1180, USA*

[b]*Faculty of Mechanical Engineering, Czech Technical University, Prague, Czech Republic*

[c]*OPTEK, Prague, Czech Republic*

[d]*WALTER, Prague, Czech Republic*

[e]*LURGI Engineering, Prague, Czech Republic*

Received 9 February 1997; received in revised form 23 December 1997

Abstract

Laser Doppler anemometry was used to measure axial and radial velocity components in a liquid flow field in the presence of dispersed beads. Index of refraction matching between the fluid (*para*-cymene) and large, spherical beads, made of polymethyl methacrylate, was essential to extract the turbulence data from the fluid phase because of the high concentration of beads. The match allowed measurements without generating noise from the surface of the beads. The measurements were obtained under transient flow conditions to avoided need for an external solids circulation loop. The resulting data were statistical and ensembled averaged for short periods during the transient experiments where the concentration could be taken as approximately constant. The concentration levels were determined from separate particle tracking velocimetry measurements, to be described in Part II. The bead density was greater than the fluid and thus wakes were created. These local areas of fluid experienced a lowering of the velocity. The turbulent fluctuation results showed that the presence of the beads extracted energy from the mean flow and transferred that energy to the turbulence. The increase of turbulent intensity was impressive along the centerline of the column where the measurements were made. The axial

* Corresponding author. Tel.: +1-614-292-2609; fax: +1-614-292-3769.
E-mail address: brodkey.1@osu.edu (R.S. Brodkey)
[1] Present address: Department of Chemical Engineering, Yonsei University, Seoul, South Korea.

PII: S0301-9322(99)00094-4

turbulent intensity of the fluid without beads was of the order of 10% and with beads, the level was increased to nearly 70%.

Keywords: Dispersion; Solid–liquid flow; Multiphase flow; IR matching; LDA; PTV

1. Introduction

Turbulence in the fluid phase in the presence of beads is different from that of a pure fluid since the motion of solid beads affects the liquid phase. For fluid–solid flow systems, a suitable model is needed to describe the interactive motions of both phases. Turbulent liquid velocity data are essential to check the validity of such models. Such modeling and the associated data are very important during unsteady operation or when the flow is turbulent. The relative local fluctuations of the solid and fluid phases play an important role for surface controlled operations such as mass transfer, kinetics and drop breakup. Such processes are important during crystallization, fluid bed operations, solids transport, jet combustion with solid fuels, gasification etc.

The present two papers are abbreviated versions. More complete pre-publication versions can be found at the URL, given in the reference list as Haam et al. (1998). The full details for the study can be found in dissertation by Haam (1996).

2. Literature review

Though there have been many attempts to describe particle–fluid dispersions, none are considered definitive. Most approaches are restricted to small particles in which the assumption of Stokes law is reasonable. Very few models have been developed for large particle dispersion under conditions where Stokes law would not be valid. The behavior of solid–liquid dispersions differs considerably from solid–gas dispersions. Often the solid–liquid phase can be treated as a non-Newtonian fluid. Such an approach is often used for slurries. Many factors associated with particle dynamics can affect the motion of particles in suspensions such as particle drag, particle non-sphericity, Brownian motion, particle rotation, agglomeration, lift, collision etc. For very dilute systems used in most studies, particle collision and agglomeration are usually not important factors.

In two phase flow, there is little information on the velocity of the two phases measured independently. The major experimental limitations are particle–probe interactions and blockage of transmitted and scattered light by the dispersed phase. The result is that most experiments were limited to dilute flow suspensions of particle volumetric concentration of less than 1.5%.

Lee and Durst (1982) performed an experimental investigation of the turbulent flow of a two-phase suspension with uniform sized particles in a vertical pipe by using laser Doppler anemometry (LDA). They used four different diameters of glass particles (100, 200, 400, and 800 μm) in an air–solid flow system. The discrimination between solid and fluid phases was based on amplitude, but they were unable to distinguish perfectly between Doppler signals of

large and small particles. They found that the large particles (400 and 800 μm) increased the turbulence in the air phase and the small particles (100 and 200 μm) decreased it. Tsuji et al. (1984) also measured the velocities of air and solid-particle by using LDA. Five different sizes of plastic particles were used which ranged from 0.2 to 3 mm. They also used a signal discrimination method to decompose the fluid and particle phases. The principle of their signal discriminator was burst signals with sufficiently large pedestal components come from large particles, while those with a small pedestal but large Doppler components come from small tracers that follow the fluid motion. They measured mean particle and air velocities across the pipe radius and turbulent intensities of air with various sizes of particles, but the local turbulent intensities of the particles were not obtained. Hestroni and Sokolov (1971) discovered that the turbulent intensity and energy spectra of the carrier fluid were changed by the presence of the droplets. They found that spectral components at high frequency and corresponding turbulent fluctuation energy were decreased by the effect of the droplets. Zisselmar and Molerus (1979) measured the turbulent intensity in methyl benzoate with small glass particles (53 μm) and found that the intensity of the turbulence was significantly damped by the solid particles. However, in the air–solid experiments by Lee and Durst (1982) and Tsuji et al. (1984) using various particle sizes and densities, showed that large particles do not decrease the turbulent intensity of the carrier fluid but increase it significantly. For liquid–solid system, Parthasarathy and Faeth (1990) and Mizukami et al. (1992) observed the same effect. Parthasarathy and Faeth (1990) studied the flow generated by uniform free falling spherical particles for water and air systems. The range of the sizes they used was from 0.5 to 2 mm. Gore and Crowe (1989) generalized the experimental data of the particle–fluid interaction and suggested that the ratio of particle size to a characteristic length scale of flow can be used as a basic parameter to predict turbulence in the particle-laden flow. They suggested that the ratio of particle diameters to turbulence scale below 0.1 suppress turbulence, in other words, damping the turbulence of the carrier fluid and above, enhances it. Hestroni (1989) used the data of Gore and Crowe and suggested that for large particles, in which the particle Reynolds number is more than 110, vortex shedding behind the particles occurs. These vortices generate more turbulence in the carrier fluid. The particles take the energy from the average velocity and dissipate the energy to higher frequencies in the fluid. It is specifically this theoretical approach that has promise of describing our experiments.

3. Experiments

Those aspects of the experiments that are in common or are essential to the LDA measurements are included in this part. The particle tracking details are given in Part II, where the individual beads were tracked by the particle tracking velocimetry (PTV) measurements.

3.1. Flow system

The vertical system was composed of a round, glass, inner column for the flow and a polymethyl methacrylate (PMMA) square outer column. The glass, flow column has a diameter of 10.2 cm and a length of 1.12 m. The PMMA square column, about 15 cm wide, was used

for minimizing the distortion and reflection of light at the surface of the inside column. The fluid was pumped through a large vertical tank, located just before the column, to disengage any bubbles before the fluid entered the working column. Instead of building a solids transport loop system, transient experiments were used. At the start of the experiment, the beads were at the bottom of the column, the pump was started, and the beads were transported upward by the flow. A screen prevented the beads from leaving the column. They were returned to bottom by turning off the pump. Many runs were made so that by using an ensemble average, statistical significant results could be obtained. Large lead balls, supported on a wire grid, formed a packed bed (15 cm in height) at the bottom of the column. The entry ensured a uniform distribution of the flow at the measuring point, which was five pipe diameters (~0.5 m) above the bed. Radial velocity distributions without beads were obtained to assure that the central region of the column is a plug flow and is not affected by the wall. Over the central 85% of the tube diameter, the average velocity varied by about 6%. The root-mean-squared (rms) velocity varied by 30% over the central 70%. The distribution plots can be found in Haam (1996) and Haam et al. (1998).

3.2. Bead preparation

Spherical molded PMMA beads were used in *para*-cymene. The available diameters were 3.18 and 4.76 mm. The density and the index of refraction of PMMA are 1190 kg/m^3 and 1.49, respectively. The shape and size of the beads are very uniform and the measured size distribution of the beads were less than 5%. Non-dyed, clear beads were used because of the requirement of a refractive index match between the beads and liquid for the LDA experiments.

3.3. Selection of index refraction matching liquid

An adequate fluid to match the index of refraction of PMMA is difficult to find since the fluid should also meet several other conditions for a turbulent flow experiment. *para*-cymene, our final choice, has a density of 860 kg/m^3, viscosity of 1.023 cP and index of refraction of 1.49. The Pyrex flow column also has an IR of 1.49. The fluid used between the flow column and the outer square column was water. Our LDA experiments were run at ambient temperature and with laser light. The exact IR values are not know to more than two places. However, the numbers are not important, what is important is that we could not see the beads in the flow during the experiments. When the small LDA particles were filtered out, the laser beams penetrated the fluid without scattering. In a later section, a statistical analysis will be presented to show that the results had minimal interferences from possible reflections at the bead surfaces.

3.4. Basic flow characteristics without beads

The fluid Reynolds number varied over a range depending upon the control valve setting. The average fluid Reynolds number was 24000. At this average flow condition, the particle Reynolds numbers for 3.18 and 4.76 mm beads were 1040 and 1550, respectively.

3.5. Experimental setup for LDA measurements

A 2 W argon ion laser system was used. Two green beams were crossed to produced a measurement volume of about 1 mm^3. The crossing volume of the two beams was positioned at the center of the column radially and at a location five times the column diameter (~0.5 m) from the bottom of the vertical column. LDA light scattering seeds were standard LDA particles ($d \sim 5$ μm). The scattered light was detected by a photo detector in a back scattering mode. The counter signal processor filtered the Doppler signals by using the condition that the seed passes through more than eight interference fringes. If the measurement was validated, it was transmitted to the on-line computer with an A/D converter and stored. The computation process to convert raw data to velocity form was made by a short conversion program.

3.6. Experimental procedure

To avoid confusion about the experiments, it is necessary to emphasize that all the experiments with beads present were transient; i.e., the system was filled with fluid, the beads were located at the bottom of the column (on top of the lead packing), the pump was started, data was gathered as the beads were transported to the top of the column, and finally the pump was turned off so the beads could settle back to the bottom of the column, ready for the next transient experiment. Thus, the solids were *not* introduced into the flow during the experiments. We chose this option because unknown effects can be introduced, if the beads were injected into the flow and because such injection systems can be costly.

4. Data, theory and discussion

4.1. The liquid velocity and time periods of the transient flow

Since each run was a time transient experiment, time periods had to be defined. In this work, we will refer to these time periods (where the concentration of beads could be assumed constant at the average concentration) as periods. This is done to emphasize that we are dealing with an average in time, not space. Thus, we use the term concentration period or subperiod. The evaluation of the velocity data was made for each subperiod of time where the flow conditions were assumed to be relatively constant. In other words, the mean flow was assumed constant with a constant concentration of beads in the given small time period. The selection of periods is somewhat arbitrary. It is necessary to make the period short enough so that the averages can represent point periods in time, but long enough so that an adequate statistical sample is obtained during the period. In this paper, the periods used have been selected to be the minimum needed for clarity of presentation.

From the PTV experiments with 15% dyed beads, the concentration of the beads in specific runs was subdivided into periods within the full time sequence. The PTV experiments are to be described further in Part II. One example of selected pictures, from the sequence used in the PTV analysis for the larger beads, is shown in Fig. 1. Based on many similar runs, the ensemble averaged concentration–time profile shown in Fig. 2 was produced. These are the

total volume concentration in percent, where it was assumed that the 15% marked beads was a constant in all periods and at all times. In Fig. 1, there are 85% of the beads not visible. For the LDA measurements, all the beads were clear and could not be seen. In Fig. 2, the periods that will be used in this paper are defined. In Haam (1996) and Haam et al. (1998), these periods are further defined and sub-divided for both size beads.

To avoid misunderstanding, we would like to digress a moment and put the present measurements into perspective with general understanding of particulate transport. From dense bed and fluidized bed technology, it is well known that there is spacial variation of concentration both on the average and instantaneously. On the average, the concentration varies near the wall of the column and instantaneously, the concentration varies everywhere,

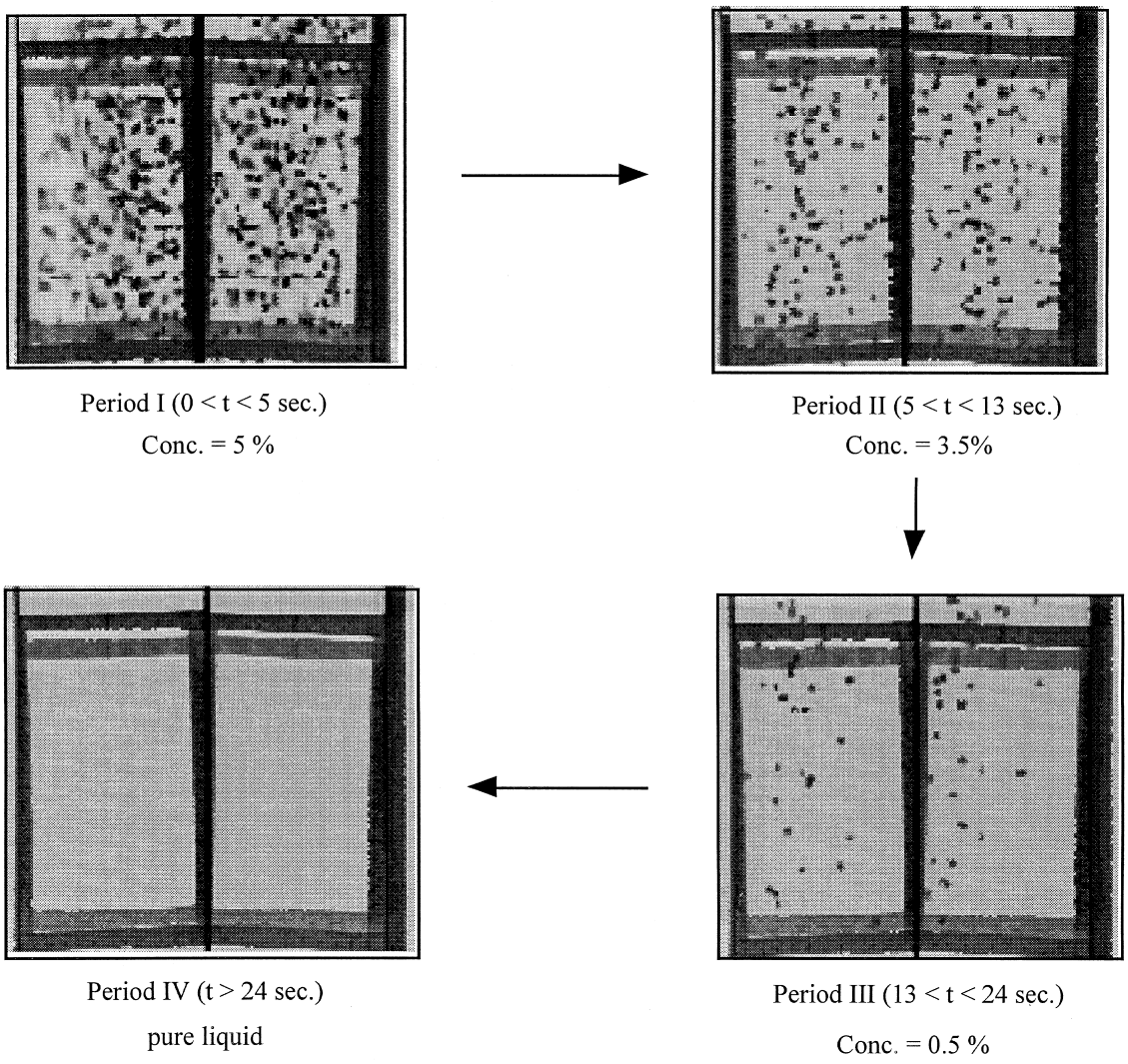

Fig. 1. Concentration of beads with time.

especially in a bubbling bed. Our statistical analysis allows us only to consider the bead flow on a global average in the area of observation (but as a function of time), as will be detailed in Part II. By averaging a large number of run, we average out any variations that occur instantaneously. We do not have measures of the spacial variation of the beads as only 15% of them were marked. On the average, the distribution appeared to us to be well distributed and uniform. In our work we can only hypothesize about the instantaneous realizations of the flow that must be the source of the enhancement of the turbulence that is observed.

The statistical evaluation of the velocity data was based on mean velocity and rms values that represent the fluctuating velocity. Histograms were made for comparisons under various conditions that depend on the bead concentrations (i.e., the time periods). The analyzes were done on both smaller and larger beads along the centerline of the column. Enough runs (more than 20 runs for each condition) were made so that an ensemble average would have meaningful statistical significance. In this paper, only the graphs for the larger beads will be shown. Many of the figures and plots not shown here can be found in Haam (1996) and Haam et al. (1998).

4.2. Characterization of the flow without beads

The flow distribution across the field has already been discussed. Further flow information without beads present is contained in this section.

4.2.1. Preliminary information for start-up transient experiment

To obtain information about the time for the fluid to achieve steady state, many time-transient LDA experiments were made (see Haam (1996) and Haam et al. (1998)). A time delay exists from the time the pump was started to the time a major change was observed. This is the time needed for the fluid in the column below the measuring point to be convected past the measuring point. During this period, the fluid (in the column and at rest) was convected as a turbulent free plug past the measuring point. Turbulence in the fluid was established

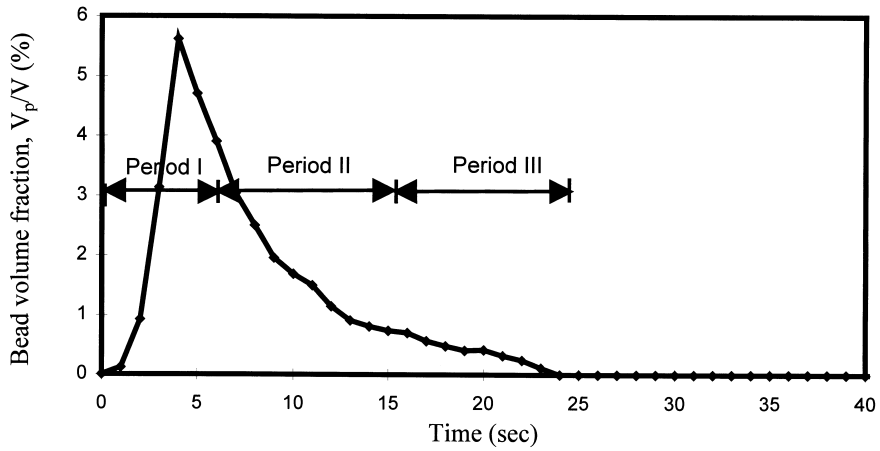

Fig. 2. Ensemble averaged concentration vs. time curve.

immediately upon passage of this starting slug. The delay time to establish the turbulence was as fast as 3 s at high velocities. The fluid was fully developed when the plug arrived at the measurement point located ~0.5 m above the entry.

4.2.2. Basic flow information without beads

In Haam (1996) and Haam et al. (1998), typical signals for both the axial and radial instantaneous velocities can be found. The axial mean and rms velocities of the flow were 0.289 and 0.033 m/s, respectively making the turbulent intensity about 10%. Our column was not typical of pipe flow as the measurement location was only five pipe diameters downstream of the pack-bed entry. The flow was nearly a turbulent plug flow with only a small region near the wall being effected by the wall. The radial mean and rms velocities were 0.6 (closed to zero) and 0.026 m/s. The rms velocities of the axial and radial component are not equal indicating that the system is not isotropic. Fig. 3 shows the number histogram for the axial velocity of the flow without beads. The x-axis of the histogram was prepared using the t-student distribution, $(U - \langle U \rangle)/s$, where U is the velocity of an individual run, $\langle U \rangle$ denotes ensemble average and s is the standard deviation. For pipe flow or a grid entry, an approximately normal distribution of the velocity is expected. A normal Gaussian distribution is also shown in the figure and the agreement with our data is excellent. The comparison suggests that an adequate statistical sample was available for this data. Note that the data is not skewed and that it is very nearly normal. The use of the mean and statistical deviation, as measured in these runs, for normalization is justified.

4.3. Confirmation of index of refraction match

We need to confirm that the index of refraction match between the beads and fluid is adequate so that the LDA signals represent fluid motions and do not include reflections from

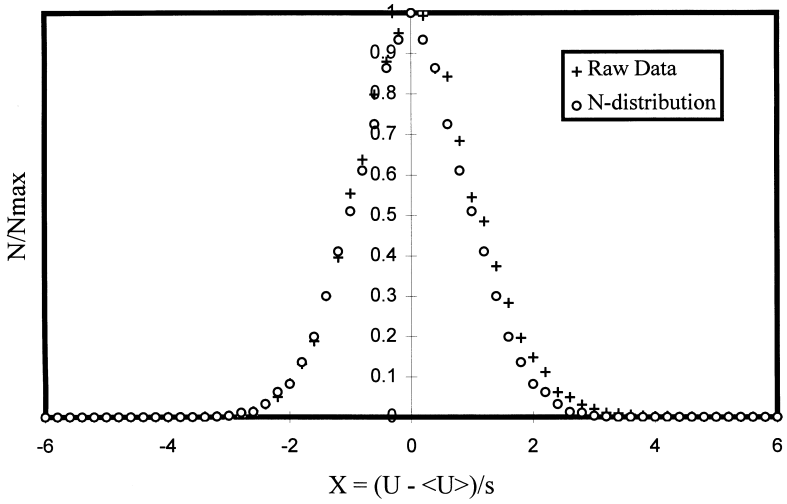

Fig. 3. Detailed number histogram, no beads, period IV ($t > 20$ s), for all axial velocity data.

the surfaces of the beads. Runs were made where we attempted to filter out the LDA particles, but with the clear matched beads still present. An example of this signal versus time is shown in Fig. 4. The contrast with the normally measured turbulent signal is marked in the total number of data samples per run time. A normal signal with the LDA particles present resulted in more than 100 times what was observed without the particles (see Haam et al., 1998). The points marked in Fig. 4 are where an actual signal was obtained. We know that if the filtration of LDA particles and the index of refraction match were perfect, there would be no signals from the flow. Fig. 4 shows that some signals were obtained. We conclude that the few measurements are either due to a few residual LDA particles or at worst from the index of refraction match being imperfect. There is no way to prove whether the flow signals are from unfiltered residual particles or from a bead effect. If we attribute the entire signal to error, the maximum contributions to the velocity data and the fluctuation energy are less than 5% or 20%, respectively. We concluded that bead reflections can be neglected or are at worst a minor error that would not change any of the conclusions to be made.

4.4. Characterization of flow with beads

Example figures for the axial and radial transient flow data for both bead sizes can be found in Haam (1996) and Haam et al. (1998). Beyond 15 s for the smaller and 20 s for the larger beads, only rarely were beads present in the test section and the measurement is characteristic of the flow without beads. When beads were present in the flow (time < 10 s), there were many large negative velocity excursions that lowered the velocity (Haam et al., 1998). During this period, when dyed beads were present for the PTV measurements, one could observe that the beads traveled downwards sometimes. Recall that the beads are non-buoyant and have a higher density than the fluid. From the results in the previous paragraph, bead reflection can be neglected and we estimated that the boundary effect can also be neglected due to it being very thin ($\approx 1 \times 10^{-4}$ m or 0.1 mm). Thus, we hypothesize that the low velocity excursions are from bead wakes. The wakes are the only source of velocities lower than that of the general fluid. There are very many beads present and each contributes a small region of negative

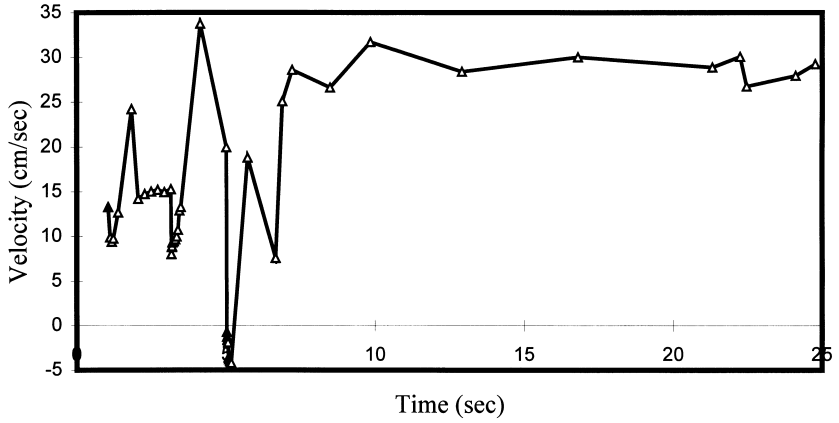

Fig. 4. Axial transient flow with beads but no LDA particles.

velocity fluctuation, which when integrated over the whole must be the source of the increased rms velocity observations. Positive excursions might result from flow between two or more close beads; however, since the fluid would tend to move with the beads, the velocity between them would rapidly adjust to the bead velocity, which is lower on the average than the fluid velocity. Fig. 5 is a sketch of the possible bead wake effects on the fluid. The generation of the wake is found behind the bead since the flow is upward and the bead is heavier than the fluid.

4.5. Histogram analysis

The most important result from the LDA data is the differences in turbulence levels in the presence and absence of beads. As described earlier, we have several bead concentration periods within each run as defined from the PTV results. To compare the flow within these different periods, histogramming was used as our main tool. Period IV, where beads were not present, was chosen as our reference basis for comparison. The x-axis of the histogram was taken as $X = (U - \langle U \rangle_{IV})/s$, where $\langle U \rangle_{IV}$ denotes the ensemble average of U during period IV when the beads were not present and s is the standard deviation. The y-axis was often normalized on the maximum value of the variable so that the maximum value plotted would be unity for all cases. Such multi-plot histograms can be confusing; thus, the histograms were smoothed using localized polynomial smoothing. The raw histograms can be found in Haam (1996) and Haam et al. (1998). Fig. 6 shows the smoothed number histogram for all axial velocities. When the time periods with beads are compared with the number histogram in

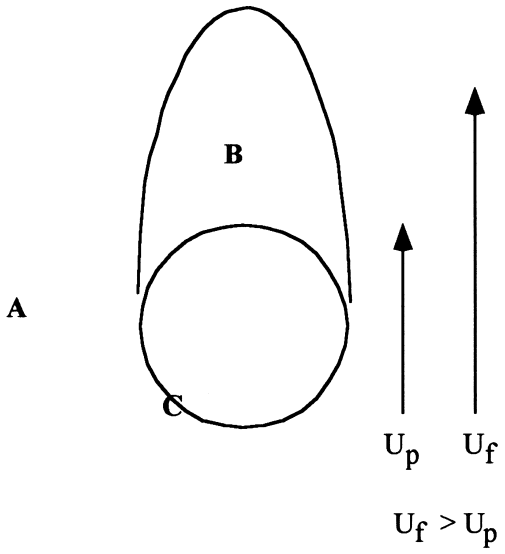

A: Fluid region away from particle wake
B: Particle wake region
C: Boundary layer

Fig. 5. Sketch of particle wake.

period IV where beads were not present (in Fig. 6 or Fig. 3), the effect of the presence of the beads on the flow can be seen. These plots show a great deal of skewness toward the negative side due to the presence of beads that can be explained by the wake effect behind the beads.

4.5.1. Analysis of the positive axial velocity segment

As can be seen from Fig. 6, the curves for different periods are similar for the positive part of the histogram ($X > 0$). This observation can be explained from the fact that the beads (heavier than the fluid) move upward at a lower velocity than the fluid and wakes are generated behind the beads. These wakes produced lower velocities and affected the negative side ($X < 0$) rather than the positive X. In our analysis of the positive segment, we replotted the results with the different periods normalized on the maximum for $X > 0$, not globally; thus, the y-axis maximum was still unity. These are not presented here because there are very similar to the positive side of Fig. 6. However, examples of these can by found in Haam (1996) and Haam et al. (1998). The segments were found to be Gaussian in shape. In this section, the data analysis will be directed toward this specific area. Since these results are normalized to unity on the y-axis and are normalized with the standard deviation on the x-axis, it is not advisable to draw conclusions at this point about the relative intensity of turbulence from the curves.

Fig. 7 shows the number histogram (n/n_{max}) and the *total fluctuation energy* during period I. The y-axis is normalized with the maximum value in this period for each item. The energy histograms are bimodal, as expected. The histogram is a measure of the *fluctuation energy* about the mean. The values are near zero when the y-axis is near zero and are high when the deviations are large for the mean. The very large negative region can be associated with the energy in the lower velocities wakes of the beads. These velocities are considerably lower than the average velocity. The positive region can be associated with the energy away from the wake between the beads. These velocities are near the average (not from zero on the x-axis) as would be expected for the flat average velocity profile that exist for this flow.

Fig. 8 is the histogram comparisons of the velocity counts for all periods. This is for the positive velocity segment ($X > 0$), but now are not normalized on the maximum values. The numbers in these figures are the velocity count per 'total run time', i.e., like a frequency.

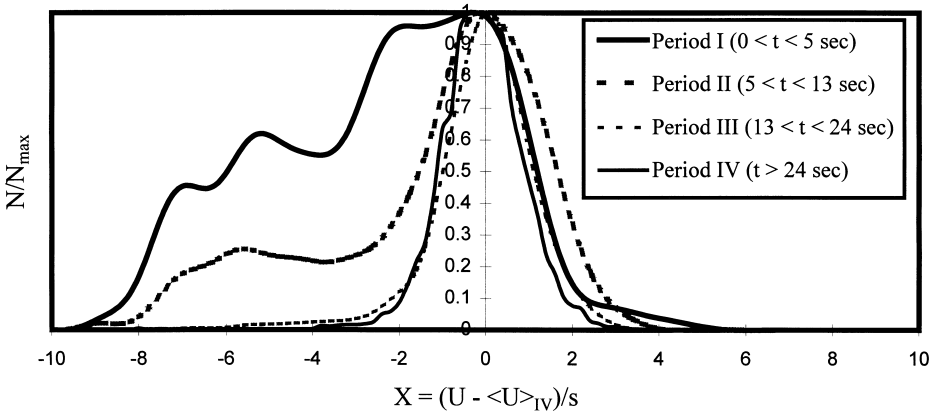

Fig. 6. Comparison of number histogram for smoothed data with beads for all axial velocities.

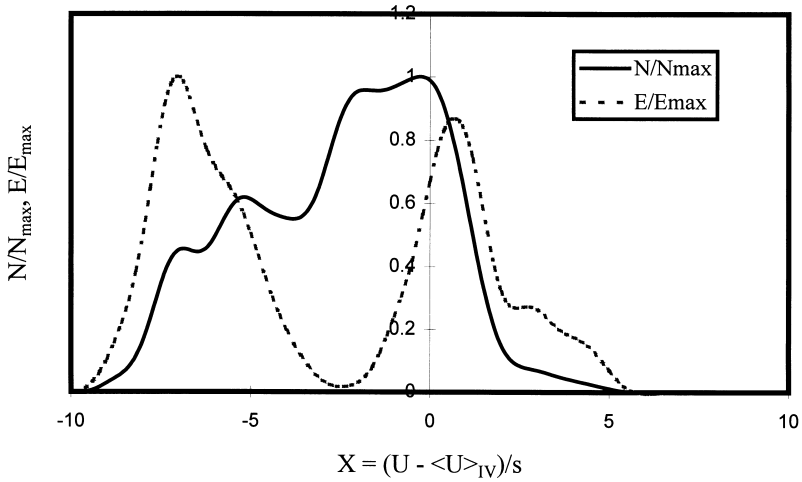

Fig. 7. Histograms of number and total fluctuation energy with beads during period I ($0 < t < 5$ s), for all axial velocities.

Periods III and IV are similar as expected, with period III showing some effect of the beads. The effect of the beads can be more readily seen in the figure for periods I and II. Because the beads are heavier than the fluid, their downward relative velocity (in the wake) reduces the number of positive excursions; i.e., period I is about 1/6 of period IV. Thus, the number of positive counts per second of run time is reduced.

Total fluctuation energy ($e \sim \sum(U - \langle U \rangle)^2$, where $\langle U \rangle$ denotes the local ensemble averaged mean velocity in the period being considered) was used to investigate the increase of the turbulence in the fluid with beads present. rms and turbulent intensity values were also determined for the overall comparisons. For a meaningful measure of the total fluctuation energies of various periods, the same total number of actual measurements (*events* at the point of measurement) in the different time periods was required. Period IV always had the highest number of events, so that the *total fluctuation energies* in other periods were multiplied by the

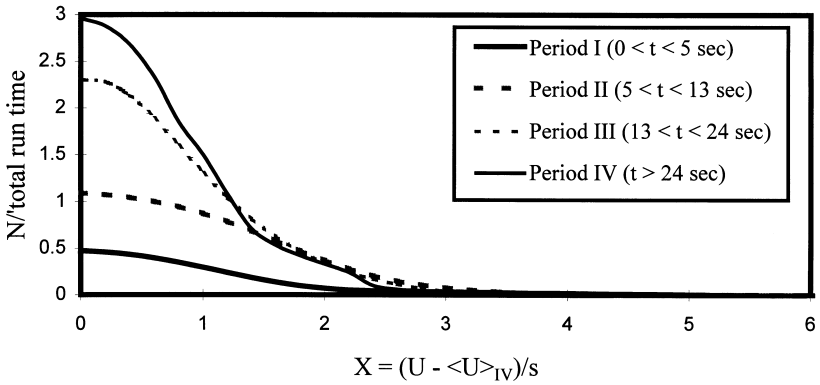

Fig. 8. Comparison of number histograms with beads for all axial positive velocities on a unit 'total run time basis'.

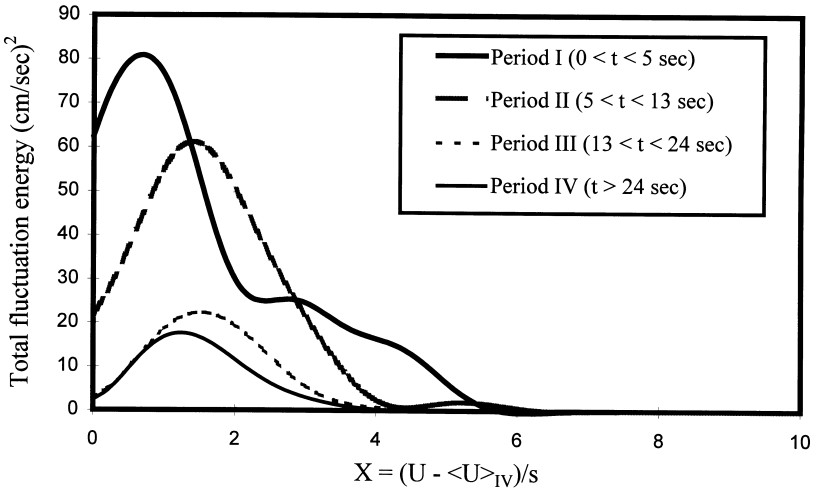

Fig. 9. Comparison of total fluctuation energy histograms with beads for all positive velocities.

ratio, 'number of events in period IV/number of events in the period being considered'. Fig. 9 is the histogram comparison of the *total fluctuating energy* on the same number of events basis. This comparison is based on the number of events at a point and is not a volume measurement. For convenience, the y-axis for the energy does not reflect the density or the factor of two. It is in reality U^2 in units of $(m/s)^2$. The results of the total fluctuation energies, rms values for the positive part of the histogram and intensities are shown in Table 1. From Fig. 9 and Table 1, we see that the total fluctuation energies with beads present in the highest concentration period (I) are clearly higher by about a factor of seven. One can conclude that the beads do strongly affect the turbulence levels in the fluid.

4.5.2. Analysis of negative and overall axial velocity part

Fig. 10 is number histogram of all axial velocities on a run second basis. The results for the smaller beads, Haam (1996), are very similar. The histogram for the various time periods are similar except that of period IV. The distribution without beads (period IV) falls off more

Table 1
Results of total fluctuation energy, rms velocity and turbulent intensity with beads for the positive axial velocities

	Total fluctuation energy $(cm/s)^2$		rms velocity (cm/s)		Turbulent intensity (%)	
	Bead diameter (cm)		Bead diameter (cm)		Bead diameter (cm)	
	0.318	0.476	0.318	0.476	0.318	0.476
Period I	1037.8	973.5	13.1	11.6	79.4	56.4
Period II	423.3	730.1	6.0	5.0	25.5	19.9
Period III	191.5	229.8	3.5	3.5	13.1	12.3
Period IV	147.4	166.4	3.2	3.4	11.8	11.0

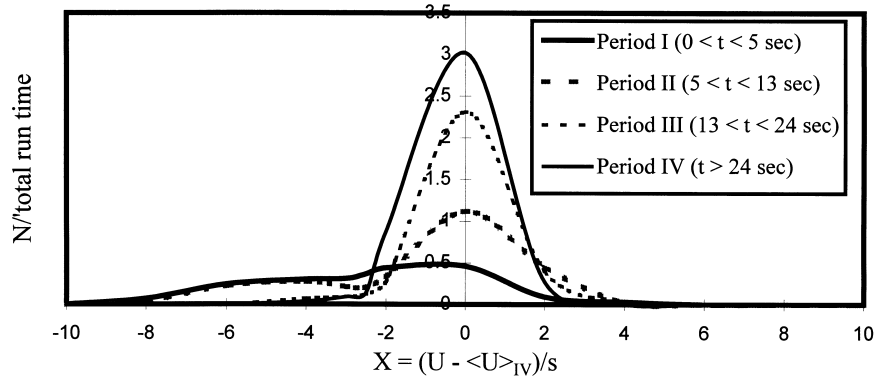

Fig. 10. Comparison of number histograms with beads for all axial velocities on a unit 'total run time basis'.

rapidly in a Gaussian manner, while the other distributions have long negative tails associated with the lower velocities that are a part of the bead wakes. The histograms are what one would expect for large negative excursions. Although the number of events may not be large in these tails, the energy associated with them could be significant.

Fig. 11 gives the *total fluctuation energy* for the entire histogram on the same number basis. Fig. 12 contain the information for the *total energy* based on the same number (not relative to an average, but the actual velocity squared without the density or the 1/2 factor). The total energy is near Gaussian for the time period without beads (IV) and is a relatively narrow distribution. For the time period with beads (I–III) the distribution is much broader and not as peaked. The maximum total energy is greater without beads. The presence of beads smooths the distribution resulting in a lower maximum but a broader shape. The fluctuating energy should reflect this observation and will be discussed next.

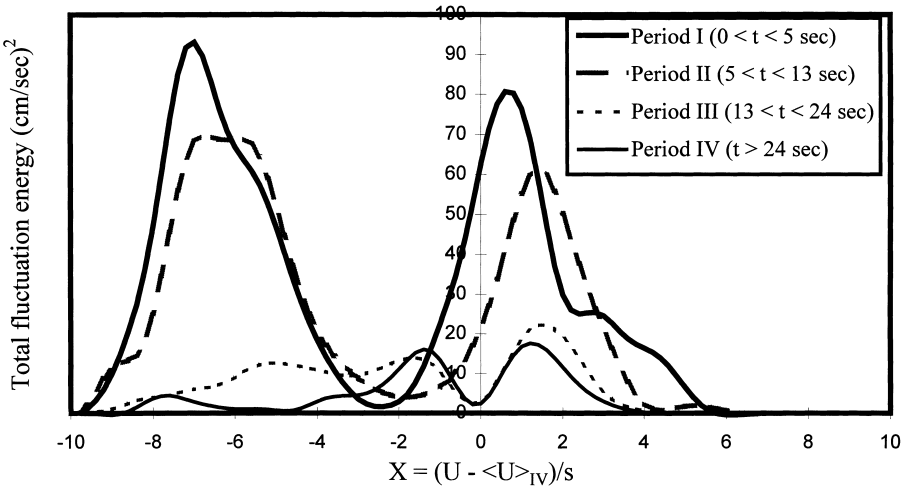

Fig. 11. Comparison of total fluctuation energy histograms with beads for all velocities.

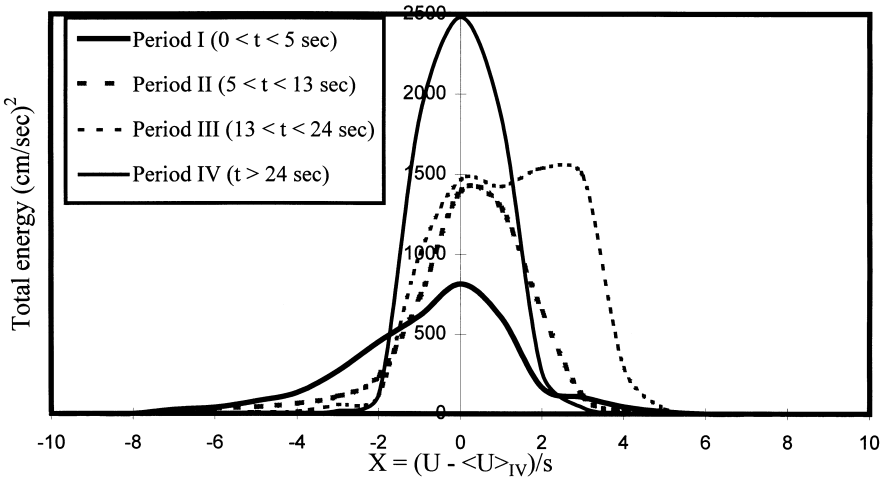

Fig. 12. Comparison of total energy histograms with beads for all velocities.

Fig. 11 shows that the fluctuation energy is greater for the higher concentration periods (I–II) than for the lower concentration ones (III–IV (no beads)) as expected from the previous results. Of course, the total fluctuation energy is a fraction of the total energy as is always the case for turbulent flows. Table 2 contains the results of the mean, rms velocities (square root form of fluctuating energy) and turbulent intensity (rms divided by mean velocity). The enhancement of the turbulence in the fluid by the beads is increased up to five times (period I) more than in the period IV where no beads are present. (If the periods are further subdivided as in Haam et al. (1998), the early subperiods are as much as seven time larger). The turbulent intensity decreases with decreasing concentration level of the beads from periods I to III. The turbulence in the periods III and IV are similar since the concentration level of the beads in period III is low (2–0.05%). From this table, we see that smaller beads can caused more turbulence than larger beads for the early periods (see also Haam et al., 1998). This observation implies that the smaller beads (but still considered large and heavy beads) interact with the fluid more actively since their mass is less and cause more turbulence than larger

Table 2
Results of mean, rms velocity and turbulent intensity with beads for all axial velocities

	Mean velocity (cm/s)		rms velocity (cm/s)		Turbulent intensity (%)	
	Bead diameter (cm)		Bead diameter (cm)		Bead diameter (cm)	
	0.318	0.476	0.318	0.476	0.318	0.476
Period I	16.55	20.75	10.74	8.75	64.89	42.17
Period II	23.91	25.22	6.57	7.94	27.48	31.48
Period III	26.63	28.43	3.34	4.41	12.54	15.51
Period IV	26.51	28.38	3.22	3.29	12.15	11.59

Table 3
Results of radial mean and rms velocity with beads

	Mean velocity (cm/s)		rms velocity (cm/s)	
	Bead diameter (cm)		Bead diameter (cm)	
	0.318	0.476	0.318	0.476
Period I	3.06	1.53	4.64	4.50
Period II	0.81	0.98	3.98	3.26
Period III	−1.37	0.81	3.06	2.84
Period IV	−0.60	0.74	2.62	3.05

beads. Hestroni (1989) suggested that for large particles, in which the particle Reynolds number is more than 110, vortex shedding behind the particles occurs. These vortices create more turbulence in the fluid. The order of particle Reynolds number for the smaller beads was 1040 and for the large was 1550.

4.5.3. Analysis of radial velocity data

Separate runs were made to measure the radial velocity component at the column centerline. The average velocity is, of course, symmetrical at the centerline. The same normalization for the x-axis was used as in the axial cases with the mean velocity in period IV, $\langle V \rangle_{IV}$, (even though it was small), and the standard deviation s. These specific figures can be found in Haam et al. (1998). They are the same type of plots as for the axial velocity. For the periods in which the beads are present, the histogram is flatter (fewer low radial velocity values) and broader (more high radial velocity values). When the beads are present, the radial component of velocity in the fluid is enhanced. Both bead sizes effect the fluid in a similar manner.

For the radial data, the *total energy* and the *total fluctuation energy* plots are also symmetrical, as expected. The time periods with beads have more total fluctuation energy than without beads; this is a reflection of the higher velocities. The positive and negative sides of the radial histograms are more symmetrical than those for the axial velocity. This is a reflection of the centerline symmetry that exists in the radial case and does not exist for the axial case. However here, because of the symmetry at the centerline for the radial measurements, the histograms clearly split into a negative and positive peaks.

Table 3 contains the radial results of mean and rms velocities for small and larger beads. The table show that the level of the turbulence is also enhanced for the radial direction by the presence of the beads.

5. Conclusions

The use of *para*-cymene as the index of refraction matching fluid for the PMMA beads was an excellent choice. In the visualization experiments, the clear beads were not visible in the *para*-cymene liquid. Under the green laser light ($\lambda = 514.5$ nm), the index match was adequate.

As a worst estimate, the beads themselves could contribute as much as 5% to the velocity or 20% to the energy; however, it is believed to be much less.

The flow was a plug flow as verified by the flat velocity distributions across the radius. Furthermore, the number histogram of the region where no beads were present showed a very near normal distribution so that the sampling conditions for LDA measurements were adequate and the velocity data were statistically meaningful.

The data obtained from LDA measurement of the axial velocity in the dispersion column with beads clearly showed that the presence of the beads caused a significant lowering of the velocity. The beads had a density greater than the fluid and created wakes behind the beads, which caused a lowering of the velocity. The lower velocities caused by the presence of the beads had long negative tails in the histograms and these tails contributed to the higher turbulence level of the fluid. The total fluctuation energy, rms velocity and turbulent intensity data from LDA measurements were compared between the periods both with and without the presence of the beads. The results showed that the presence of the beads extracted energy from the mean flow and provided that energy to the fluctuation turbulence level. The increase of turbulent intensity was impressive along the centerline of the dispersion column where the measurement was made. The axial turbulent intensity of the fluid without beads was 12% and with beads, the level was increased to 69% for the smaller 1/8 in. beads and 49% for larger 3/16 in. beads. The turbulence along the radial direction was also enhanced by the presence of the beads. The normalization used for the radial turbulent intensity was the rms value, since the radial mean velocity was close to zero. The rms value of the period without beads was about 0.030 m/s and increased up to 0.046 m/s for smaller beads and 0.08 m/s for larger ones. The presence of beads affected the axial velocities much more than radial velocities. However, the enhancements on the radial direction were not small. From the results of Tables 1–3, the bead size effect can be seen. The smaller beads, which are small but still considered as large particles, enhanced the turbulence for the axial direction more than the larger ones in the early periods. The histograms for the periods where beads were present showed a great deal of skewness toward the negative side due to the wakes behind the beads. For the total fluctuation energy, these regions had long tails. However, the positive part of the distribution that could be associated with the pure fluid was near Gaussian. Although the number of events may not be large in the negative tails, the energy associated with them could be significant.

Acknowledgements

The authors wish to thank the National Science Foundation for an International Cooperative Grant with the Czech Republic for the support of this work. Without this mutual effort of exchange of researchers, the laser Doppler study would most certainly take far longer. The support of the Department of Chemical Engineering for S.J. Haam throughout the two periods that he studied in Columbus is also greatly appreciated.

References

Gore, R., Crowe, C.T., 1989. Effect of particle size on modulating turbulent intensity. Int. J. Multiphase Flow 15, 279–285.

Haam, S.J., 1996. Multiphase research on solid–liquid dispersion. Ph.D. dissertation. Department of Chemical Engineering, The Ohio State University.

Haam, S.J., Brodkey, R.S., Fort, I., Klaboch, L., Placnik, M., Vanecek, V., 1998. Laser doppler anemometry measurements in an index of refraction matched column in the presence of dispersed beads. (http://www.er6.eng.ohio-state.edu/~brodkey/curnot.htmlx).

Hestroni, G., Sokolov, M., 1971. Distribution of mass, velocity and intensity of turbulence in a two-phase turbulent jet. Trans. ASME J. Appl. Mech 38, 315–327.

Hestroni, G., 1989. Particles–turbulent interaction. Int. J. Multiphase Flow 15, 735–747.

Lee, S.L., Durst, F., 1982. On the motion of particles in turbulent flow duct flows. Int. J. Multiphase Flow 8, 125–146.

Mizukami, M., Parthasarathy, R.N., Faeth, G.M., 1992. Particle-generated turbulence in homogeneous dilute dispersed flows. Int. J. Multiphase Flow 18, 397–412.

Parthasarathy, R.N., Faeth, G.M., 1990. Turbulence modulation in homogeneous dilute particle-laden flow. J. Fluid Mech 220, 485–537.

Tsuji, Y., Morikawa, Y., Shiomi, H., 1984. LDV-measurements of air–solid two-phase flow in a vertical pipe. J. Fluid Mech 120, 358–409.

Zisselmar, R., Molerus, O., 1979. Investigation of solid–liquid jet pipe flow with regard to turbulence modulation. Chem. Eng. J 18, 233–239.